SCIREA Journal of Civil Engineering and Building Construction
http://www.scirea.org/journal/CEBC
May 23, 2023
Volume 8, Issue 1, February 2023
https://doi.org/10.54647/cebc560119

Effect of Mortar Bleeding on Surface Layer Permeability After Hardening

Yuto Horiuchi[1], Keita Hayashi[2], Ayumu Yasue[3], Shigeru Fujimori[4], Toshitsugu Inukai[5,*]

[1]Advanced Course of Interdisciplinary Technology Development, National Institute of Technology, Gifu College, Gifu Prefecture, Japan

[2]Residential Division, Urban Construction Department, Gifu Prefectural Government, Gifu Prefecture, Japan

[3]Institute of Technology, Shimizu Corporation, Tokyo Metropolis, Japan

[4]Department of Architecture, School of Engineering, Daido University, Aichi Prefecture, Japan

[5]Department of Architecture, National Institute of Technology, Gifu College, Gifu Prefecture, Japan

*Corresponding author: Toshitsugu Inukai, *inukai@gifu-nct.ac.jp*

Abstract

In this study, we examined evaluation methods based on hydraulic flux measured with the permeability-testing device GWT-4000 and its relationship with bleeding, which affects surface layer quality. We also analyzed the effects on bleeding of the permeability distribution in the height direction of a sample. The results showed that the hydraulic flux q_{600} of the driving surface was higher than that of the bottom surface. Moreover, we could determine the bleeding effects. The hydraulic flux q_{600} of the bottom surface was strongly correlated to the amount of bleeding in the small container. It was also found that the hydraulic flux q_{600} only captured the

permeability of the top-most layer, did not capture the effects due to the mix proportion factors in the height direction, and was primarily affected by the mold interface.

Keywords: *Bleeding, surface layer, permeability, permeability test, GWT-4000, hydraulic flux*

1. Introduction

Bleeding is a factor that reduces the surface layer quality of concrete structures. The water/cement ratio of the upper layer increases due to bleeding; thus, the compression strength of the upper layer decreases compared to that of the lower layer [1]. Moreover, studies have reported that an increase in the amount of bleeding increases the air permeability coefficient of the upper layer and affects the air permeability distribution of the side surface layers in the height direction [2].

Furthermore, degradation factors penetrating from the exterior affect the durability of reinforced concrete structures; thus, these structures are often evaluated using the mass transfer resistance of the surface layer, with the permeability test considered as one of these evaluation methods. We have previously examined an evaluation method relying on the permeability test using a commercially available permeability- testing device, GWT-4000. Permeability tests using this testing device are non-destructive; thus, the test does not damage the structure and can also be applied to both horizontal and vertical surfaces. Therefore, establishing such an evaluation method can enable its use as a testing method for evaluating the mass transfer resistance of the surface layers of actual structures. A previous study [3] confirmed, from experimental results considering the mix proportion as a factor, that permeability in the surface layer could be evaluated using the hydraulic flux q600 determined 600 s from the start of measurements. However, improving the reliability of this evaluation method requires a detailed examination of its relationship with bleeding, which affects the material quality distribution in the upper layer and in the height direction.

As a preliminary step to examine the effects of concrete bleeding on the permeability of surface layers after hardening, in this study, a mortar was selected as a sample and the effect of mortar bleeding (considering the mix proportion as a factor) on the permeability of a surface layer after hardening was evaluated. The effects of bleeding on the permeability

distribution in the height direction were examined from the test results of the driving surface, upper side surface, lower side surface, and bottom surface. The amount of water absorbed through natural absorption was also measured before the permeability tests. The 10-minute natural absorption amount was also discussed.

2. The effect of water/cement ratio on hydraulic flux and bleeding amount (Experiment 1)

2.1. Experimental factors

The experimental factors were four water/cement ratio levels (50, 55, 60, and 65%).

2.2. Mortar material and mix proportion

Table 1 shows the mortar materials used in this study, while Table 2 shows the mortar mix proportions. Mortar materials and mix proportions were fixed for all cases to clarify the effects due to the water/cement ratio. The air amount and flow value were both adjusted to fall within a fixed range.

2.3. Experimental methods

2.3.1. Mortar mixing and flow tests

The mortar mixing and flow tests were conducted according to JIS R 5201, “Physical Testing Methods for Cement (10.4.3. Mixing Methods, and 11. Flow Test)”.

Table 1. Mortar materials (Experiment 1 and 2)

Materials	Type	Notes	Symbol
Cement	Ordinary Portland cement	Density:3.16 g/cm^3 Specific surface area:3480 cm^2/g	C
Fine aggregate	Dried silica sand (No.4, No. 5)	Absolute dried density:2.54 g/cm^3 Mixing ratio 1:1	S
Chemical admixture	High-performance AE water reducing agent	Main component: Polycarboxylic acid copolymer	AD
Water	Tap water	—	W

2.3.2. Air content tests on fresh mortar

For the air content of the mortar, unit mass was measured according to JIS A 5002, “Lightweight Aggregates for Structural Concrete (5.12.d. Measurement of Unit Mass of Mortar)” and calculated according to JIS A 1116, “Method of Test for Unit Mass and Air Content of Air Content of Fresh Concrete by Mass Method (6.2. Air Content)”.

2.3.3. Mortar-bleeding tests

Mortar bleeding tests were conducted using the following procedure, based on JCI-S-015-2018, “Method of Test for Bleeding of Concrete Using Small Container.”.

The sample was driven into a test container (inner diameter: 125 mm, inner height: 250 mm) in two layers. The sample surface was leveled with a trowel so that it would be a smooth surface with a minimum amount of work, immediately after which time recordings were started. The test container was placed on a non-vibrating horizontal table and covered with a lid during the tests to prevent the escape of moisture. The bleeding water was pipetted out every 30 min from the initial time of recording until no bleeding was observed. The pipetting of the water was facilitated by tilting the container two minutes before pipetting by placing a block so that the inclination angle would be 11.5°, as shown in Figure 1. The container was gently returned to its original horizontal position after the water was pipetted. The pipetted water was recorded up to 1 mL by mass. The masses of the container and sample were immediately measured after no bleeding was observed. The bleeding amount of the small container was calculated using equation (1).

Table 2. Mix proportion of mortar (Experiment 1)

No.	W/C	Air (%)		Flow value		S/C	Unit weight (kg/m^3)			
	(%)	Target	Measured	Target	Measured	(wt)	C	W	S	AD
1	50	8±2	9.0	190±20	182	2.53	508	254	1284	0.72
2	55		7.6		190	2.68	479	263		0.52
3	60		7.6		202	2.84	452	271		0.55
4	65		7.2		203	3.00	428	278		0.23

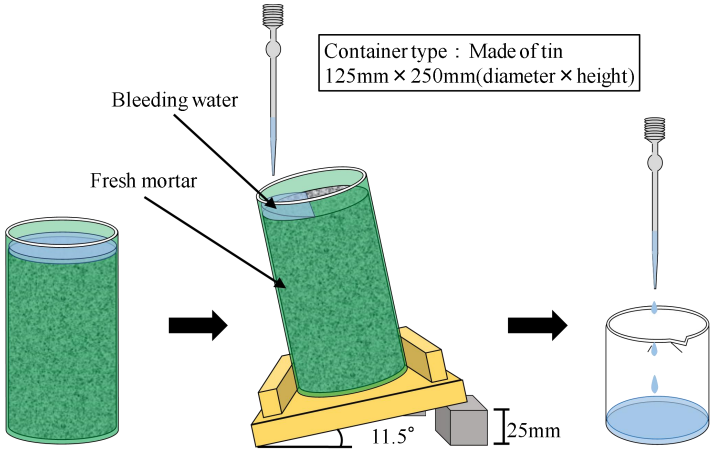

Figure 1. Small-container bleeding test method (Experiments 1and 2)

2.3.4. Permeability test of hardened mortar surface layer

Permeability tests of the hardened mortar surface layer were conducted according to the following procedure.

Mortar samples with a material age of 3 months after air curing at 28 days of standard water curing (length 100 mm×width 100 mm×height 200 mm) were placed on the GWT-4000 with the measurement position facing upwards, as shown in Figure 2. The measurement positions were set as the four locations of the driving surface, upper side surface, lower side surface, and bottom surface, as shown in Figure 3. Water was injected into a pressure chamber (cross-sectional area 3018 mm^2), after which the chamber was lightly tapped with a wooden mallet to remove air bubbles. Natural water absorption was conducted for 10 min, which was determined by measuring the water surface displacement inside the injection cup (inner diameter of 34.8 mm) using a laser displacement meter for 10 min immediately after completing the water injection. The amount of natural water absorption was calculated using equation (2), based on the measured displacement. The amount of natural water absorption was measured on the upper surface of each sample.

The lid was closed with a wrench after completing natural water absorption, and the chamber was pressurized to 50 kPa. The constant water pressure could be obtained by replacing the permeated amount with the pushed amount from the micrometer, and the permeability could be obtained by replacing the reading value of the micrometer with the permeated amount. Therefore, the measurable range was up to the maximum micrometer value of 25 mm,

$$B_q(\phi\,125) = \frac{V}{A} \tag{1}$$

Notes; $Bq(\phi\,*)$: bleeding aount of the small container (cm^3/cm^2)

$\phi\,*$: inner diameter of the container (replace * with the value displayed in mm)

V: water volume due to bleeding accumulated until the final time (cm^3)

A: area of the upper surface of the sample (cm^2)

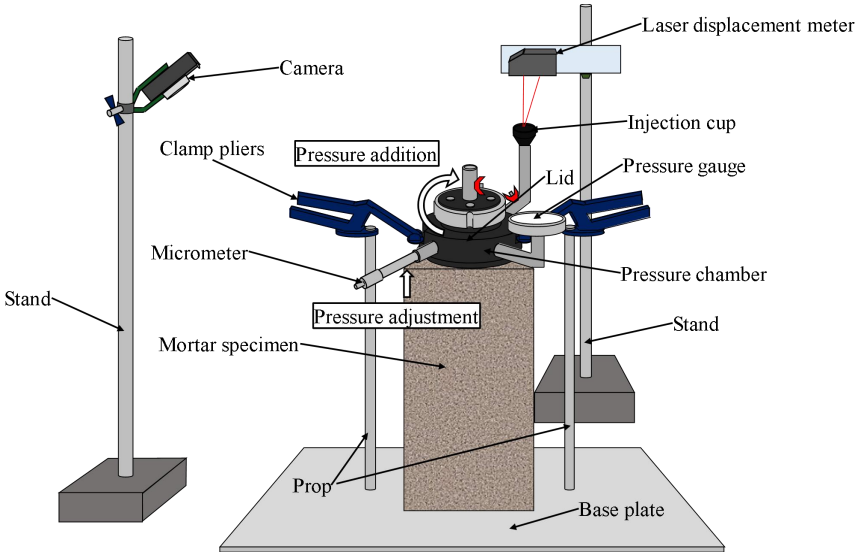

Figure 2. Driving and bottom surfaces permeability test conditions (Experiments 1and 2)

which was 1.965 mL when converted to permeability. The measurement time in this test was set to 15 min or the time when the permeated amount reached 1.965 mL. Moreover, the micrometer scale was photographed with a digital camera every 30 s. The photographs taken after the end of the tests were used to calculate the permeability from equation (3), and the hydraulic flux from equation (4). The hydraulic flux represents the hydraulic conductivity from the starting time of permeation to time t, and permeability was evaluated by the hydraulic flux q_{600} determined 600 s after starting permeation when a correlation was confirmed between the hydraulic flux and elapsed time.

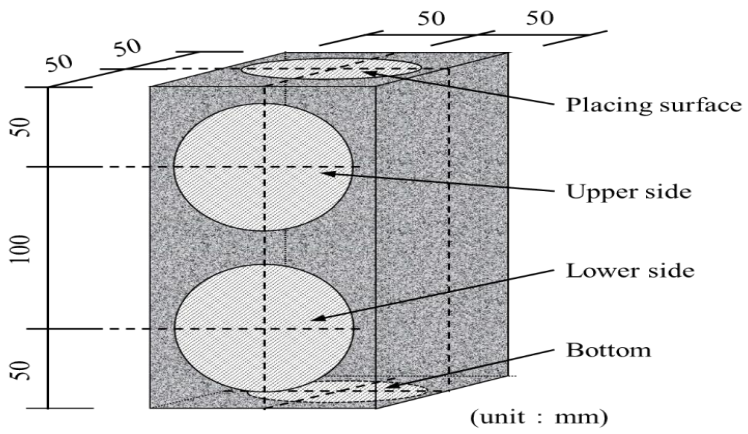

Figure 3. Measurement locations of the permeability test (Experiments 1and 2)

$$V_{nt} = \frac{x \cdot a}{A} \tag{2}$$

Notes; V_{nt}: the amount of natural water absorption at time t (ml/m^2)
x: water surface displacement at time t (cm)
a: cross-sectional area of the injection cup (cm^2)
A: cross-sectional area of the pressure chamber (m^2)

$$V_t = a(g_1 - g_2) \tag{3}$$

Notes; V_t: the amount of natural water absorption at time t (ml/m^2)
a: cross-sectional area of the injection cup (cm^2)
g_1: cross-sectional area of the pressure chamber (m^2)
g_2: cross-sectional area of the pressure chamber (m^2)

$$q_t = \frac{V_t \cdot t}{A} \tag{4}$$

Notes; q_t: the hydraulic flux at time t (ml/m^2/s)
V_t: permeated amount at time t (ml)
A: cross-sectional area of the pressure chamber (m^2)
t: elapsed time from the start of permeation (s)

2.4. Experimental results and discussion

2.4.1. Effect of water/cement ratio on the bleeding amount of small container

Figure 4 shows the relationship between the amount of bleeding in the small container and the water/cement ratio. The linear regression equation and its correlation coefficient r are also shown in the figure. An increase in the water/cement ratio tends to increase the bleeding

amount of the small container, and a strong correlation was observed between the amount of bleeding in the small container and the water/cement ratio.

2.4.2. Effect of water/cement ratio on the amount of natural water absorption

Figure 5 shows the relationship between the amount of natural water absorption on the upper side surface and the elapsed time. An increase in the water/cement ratio tends to increase the amount of natural water absorption, which was the same tendency as the amount of absorbed water with the SWAT method previously reported [4].

2.4.3. Effect of water/cement ratio and measurement position on hydraulic flux

Figure 6 shows the relationship between the hydraulic flux and the elapsed time. Exponential approximation equations and correlation coefficient r are also shown in the figure. Strong correlations can be seen between the hydraulic flux and the elapsed time for all water/cement ratios.

Figure 7 shows the relationship between the hydraulic flux q_{600} and the measurement position.

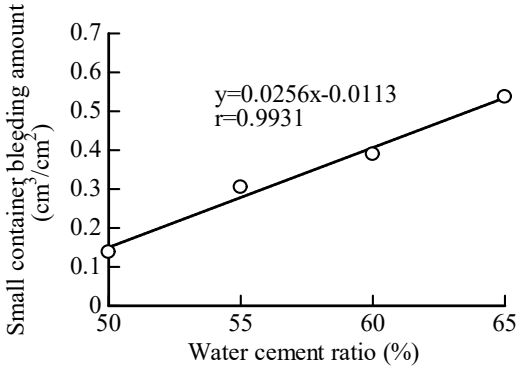

Figure 4. Relationship between the bleeding amount of small container and the water/cement ratio (Experiment 1)

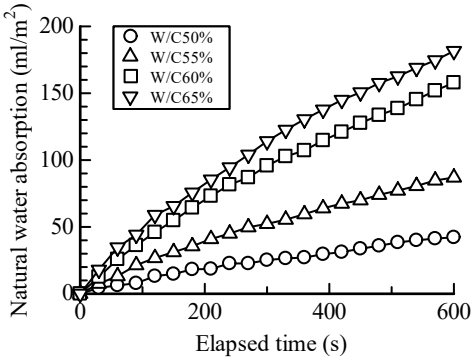

Figure 5. Relationship between the amount of natural water absorption and the elapsed time (Experiment 1)

The hydraulic flux q_{600} of the driving face was higher than that of the bottom surface for each water/cement ratio. This result indicated that the structure after hardening became porous in the upper layer and dense in the bottom layer due to bleeding. Besides, focusing on the height direction, the hydraulic flux q_{600} of the bottom side surface was higher than that of the upper side surface at the water/cement ratio of 50%. However, there were no major ifferences in the hydraulic flux q_{600} of the bottom, lower side, and upper side surfaces at a water/cement ratio of 55%. These results follow a similar tendency of a previous report [5] and indicate that the air and water permeability of the sample side surfaces were not necessarily proportional to the driving height, with the upper

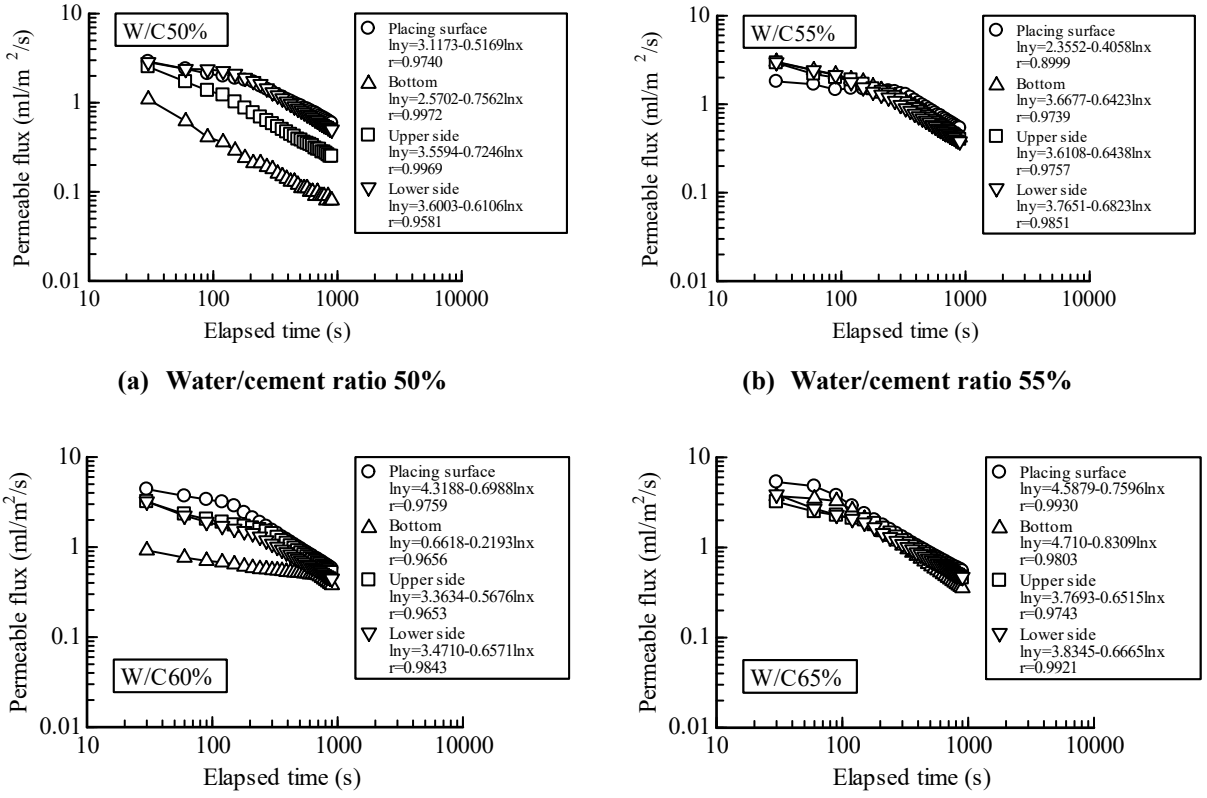

(a) Water/cement ratio 50%

(b) Water/cement ratio 55%

(c) Water/cement ratio 60%

(d) Water/cement ratio 65%

Figure 6. Relationship between the hydraulic flux and the elapsed time (Experiment 1)

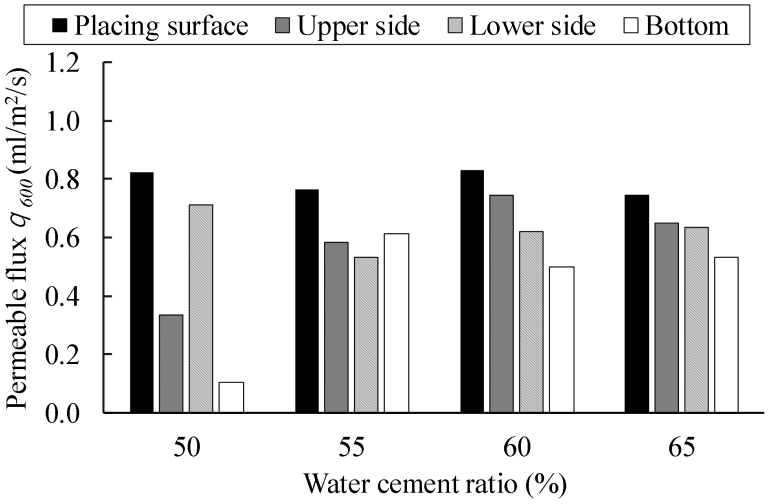

Figure 7. Relationship between the hydraulic flux q_{600} and the measurement position

layer being significantly affected by bleeding. It has also been reported [6] that the interface between the mold and the sample became a water path, and free water moved along the mold surface. Therefore, we conducted permeability tests using coloring liquid to clarify the permeable depth evaluated in this test. Permeability tests were conducted on the driving surface of the 45% water/cement ratio test until the permeated amount was 1.965 mL for the 50 kPa pressure condition. Photograph 1 shows the test cross-section after the permeability tests. As seen in the photograph, the maximum penetration depth was approximately 6 mm, and the permeability tests using GWT-4000 can be said that only evaluate the top-most layer. In other words, the hydraulic flux q_{600} determined on the side surface of the sample is thought to be heavily affected by the water path produced at the interface of the mold and sample, as well as the free water retained in the mold surface. Therefore, the results showed that it is difficult to determine the permeability distribution in the height direction accurately under the conditions where the driving height was 200 mm using these test methods. When focusing on the hydraulic flux q_{600} in the driving surface, a roughly similar value was seen regardless of the water/cement ratio. This result was likely due to the effect of smoothing out with the trowel. It was thought that the result was because a virtually identical driving surface quality was evaluated due to the homogeneous trowel smoothing conducted in this test, where the top-most layer was evaluated. However, except for the 55% water/cement ratio, an increase in the water/cement ratio also tends to increase the hydraulic flux q_{600} in the bottom layer. Therefore, the hydraulic flux q_{600} was roughly affected by the water/cement ratio in the bottom layer, where there is no trowel finishing effect.

2.4.4. Relationship between hydraulic flux and the amount of bleeding in the small container

Figure 8 shows the relationship between the hydraulic flux q_{600} of the driving surface and the bottom surface and the bleeding amount of the small container. The exponential approximation equation and correlation coefficient r are also shown in the figure. The hydraulic flux q_{600} was roughly equal across different bleeding amounts of the small container for the driving surface, and no clear trend was observed. However, an increase in the bleeding amount of the small container tends to increase the hydraulic flux q_{600}, as well as in the bottom surface, and the correlation coefficient r for this case was higher than that for the driving surface.

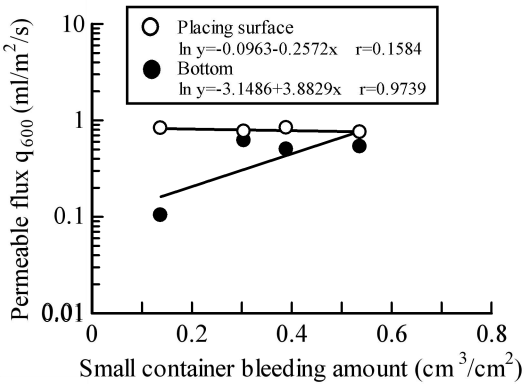

Figure 8. Relationship between the hydraulic flux q_{600} and the small container bleeding amount in the driving and bottom surfaces (Experiment 1)

3. Effect of unit water amount on hydraulic flux and bleeding amount (Experiment 2)

3.1. Experimental factors

The experimental factors were four unit water levels (259, 266, 273, and 280 kg/m3).

3.2. Mortar material and mix proportion

The mortar material used was the same as that used in Experiment 1. Table 3 shows the mortar mix proportions.

3.3. Experimental methods

The experimental methods were similar to that in Experiment 1.

3.4. Experimental results and discussion

3.4.1. Effect of unit water amount on the bleeding amount of small container

Figure 9 shows the relationship between the bleeding amount of the small container and the unit water amount. The linear regression equation and correlation coefficient *r* are also shown in the figure. The bleeding amount of the small container greatly increases from the unit water amount of 259 to 266 kg/m^3, and remains virtually constant from 266 to 280 kg/m^3.

Table 3. Mix proportion of mortar (Experiment 1)

No.	W/C	Air (%)		FL		S/C	Unit weight (kg/m^3)			
	(%)	Target	Measured	Target	Measured	(wt)	C	W	S	AD
1	55	8±2	7.6	190±20	195	2.76	471	259	1300	0.91
2			7.5		199	2.63	484	266	1273	0.51
3			6.6		195	2.50	497	273	1243	0.22
4			6.4		198	2.39	509	280	1217	0.00

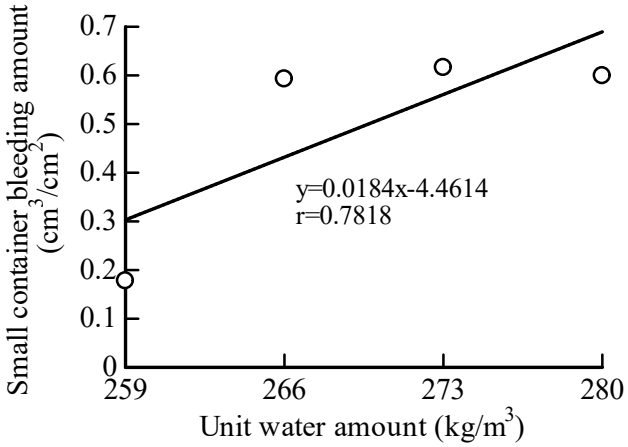

Figure 9. Relationship between the bleeding amount of small container andthe unit water amount (Experiment 2)

3.4.2. Effect of unit water amount on the bleeding amount of natural water absorption

Figure 10 shows the relationship between the amount of natural water absorption on the upper side surface and elapsed time. An increase in the unit water amount also tends to increase the

amount of natural water absorption, while a decrease in the unit fine aggregate (impermeable material) amount increases the unit water amount.

3.4.3. Effect of unit water amount and measurement position on hydraulic flux

Figure 11 shows the relationship between the hydraulic flux and the elapsed time.

The exponential approximation equation and correlation coefficient r are also shown in the figure. A strong correlation can be seen between the hydraulic flux and the elapsed time across all unit water amounts.

Figure 12 shows the relationship between hydraulic flux q_{600} and measurement position.

The hydraulic flux q_{600} on the driving surface presented a higher value than that of the bottom surface for all unit water amounts. Similar to Experiment 1, this result indicated that the structure after hardening had a porous upper layer and a dense lower layer. Moreover, focusing on the height direction, the hydraulic flux q_{600} on the bottom side surface was higher than that on the upper side surface at unit water amounts of 273 and 280 kg/m^3. Similar to Experiment 1, this result was thought to be due to the effect of the water path formed at the interface between the mold and the sample, as well as the free surface retained in the mold surface. Furthermore, no clear trends the unit water amount were observed when focusing on the hydraulic flux q_{600} of the driving surface. Similar to Experiment 1, this was thought to be due to the quality of the driving surface, which had become virtually uniform due to homogeneous trowel finishing, that was evaluated in this test, which evaluated the top-most layer of the sample. However, the hydraulic flux q_{600} also tended to increase as the unit water amount increased in the bottom surface. Therefore, the hydraulic flux q_{600} was thought to be affected by the unit water amount for the bottom surface, where there was no trowel finishing effect.

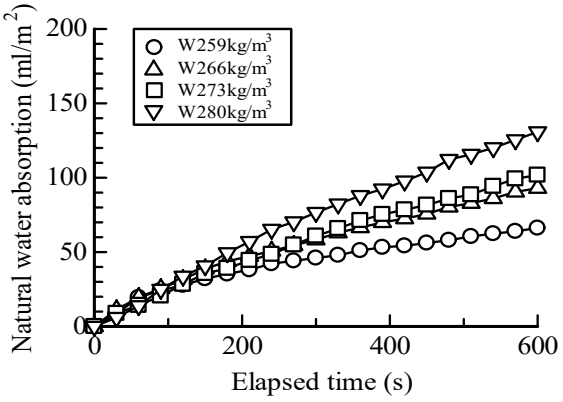

Figure 10. Relationship between the hydraulic flux and the elapsed time (Experiment 2)

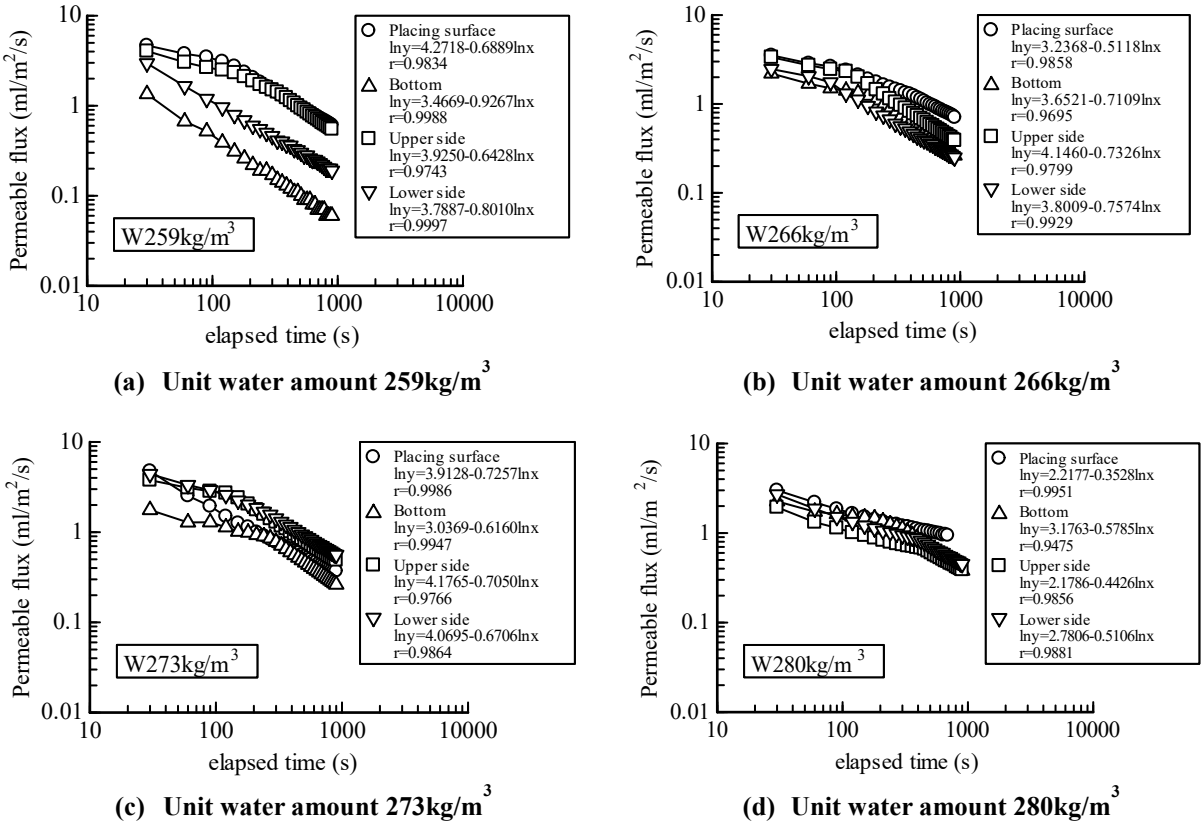

Figure 11. Relationship between the hydraulic flux and the elapsed time (Experiment 2)

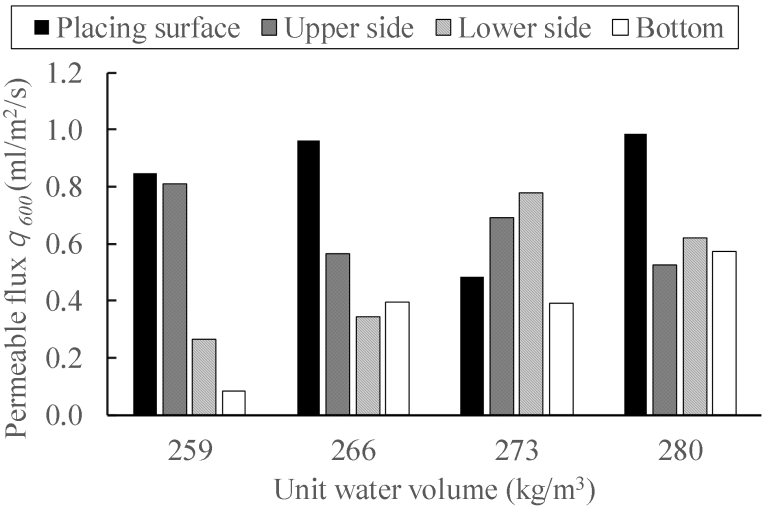

Figure 12. Relationship between the hydraulic flux q_{600} and the measurement position (Experiment 2)

3.4.4. Relationship between hydraulic flux and the amount of bleeding in the small container

Figure 13 shows the relationship between the hydraulic flux q_{600} of the driving surface and the bottom surface, and the bleeding amount of the small container. The exponential

approximation equation and correlation coefficient r are also shown in the figure. The hydraulic flux q_{600} was roughly equivalent across all bleeding amounts of the small container in the driving surface, and no clear trends were observed. However, the hydraulic flux q_{600} also tended to increase in the bottom surface as the bleeding amount of the small container increased. Moreover, a strong correlation was observed between the hydraulic flux q_{600} and the bleeding amount of the small container.

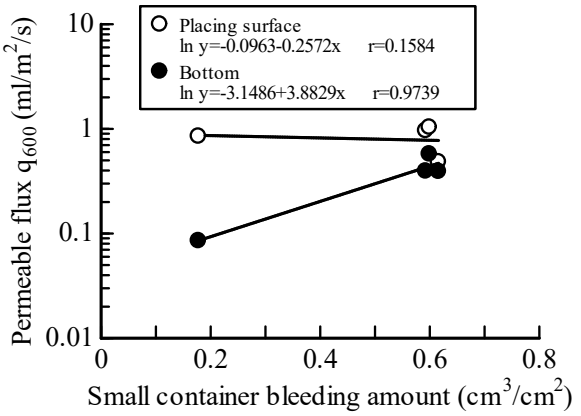

Figure 13. Relationship between the hydraulic flux q_{600} and the small container bleeding amount in the driving and bottom surfaces (Experiment 2)

4. Conclusion

The following findings were obtained from these experimental results.

1. The water/cement ratio and unit water amount affect the amount of natural water absorption.

2. The hydraulic flux due to q_{600} of the permeability testing machine GWT-4000 only captured the permeability of the top-most layer.

3. The hydraulic flux q_{600} in the driving surface was higher than that in the bottom surface, and the effects of bleeding were captured.

4. The hydraulic flux q_{600} of the sample side surface was heavily affected by the water path formed at the interface between the mold and the sample; thus, the distribution in the height direction was not properly captured in the scope of these experiments.

5. A strong correlation was observed in the scope of these experiments between the hydraulic flux q_{600} of the bottom surface and the bleeding amount of the small container.

In the future, we would like to study the relationship between the amount of natural water absorption and the hydraulic flux q_{600}, as well as the relationship between the hydraulic flux q_{600} due to the amount of natural water absorption and the hydraulic flux q_{600} due to GWT-4000.

Acknowledgements

This research was funded in part by the 2019 Koshiyama Science & Technology Research Grant (principal investigator Toshitsugu Inukai). We would like to express our gratitude for this funding.

We would like to thank Editage (www.editage.com) for English language editing.

References

[1] M. Hoshino and T. Tomabechi (1980). Relationship between bleeding phenomena and the strength of each concrete section: II. Strength of each sample section and bleeding water amount. Summaries of Technical Papers of the Annual Meeting of the Architectural Institute of Japan, 55, 55–56.

[2] K. Hayakawa and T. Kato (2012). Effect of mix proportion and construction method on the quality of cover concrete. Journal of JSCE E2, 68-4, 399-409.

[3] K. Hayashi, A. Yasue, T. Inukai and S. Fujimori (2019). Research on permeability evaluation methods using a pressurized permeability testing device and the effect of mix proportional factors on the permeability of a hardened mortar surface layer. Proceedings of the Japan Concrete Institute, 41-1, 533-538.

[4] N. Ikawa, Y. Tamaoka and A. Hosoda (2018). Fundamental study on evaluation criteria of cover concrete quality of concrete structures by surface water absorption test. Proceedings of the Japan Concrete Institute, 29, 101-109.

[5] Japan Concrete Institute (2017). Research committee report on bleeding control for improving durability of structures, 37-38.

[6] T. Inukai, S. Hatanaka, N. Mishima and R. Kaneko (2005). Experimental study on bleeding behavior of free water in mortar based on a visible evaluation method. Transactions of AIJ, 70-590, 1-7